

## Unsteady axisymmetric turbulent boundary layer on a slender body of revolution

M. KUMARI and G. NATH (BANGALORE)

THE UNSTEADY incompressible turbulent boundary-layer flow over a slender body of revolution has been studied using an eddy-viscosity model for the Reynolds shear stress. The unsteadiness in the flow field is introduced by the free stream velocity which varies with time. The nonlinear partial differential equation with three independent variables governing the flow has been solved numerically using a finite-difference scheme developed by Keller. The free stream velocity is found to exert strong influence on the characteristics of the flow within the boundary layer. The phase angle between wall shear and fluctuating free stream velocity is much smaller than the phase angle between displacement thickness and fluctuating free stream velocity. The skin friction coefficient decreases with the streamwise distance or transverse curvature parameter whereas the Reynolds number increases. The transverse curvature strongly affects the phase angle between wall shear and fluctuating free stream velocity, but its effect on the phase angle between displacement thickness and fluctuating free stream velocity is small.

Omówiono problem turbulentnego nieściśliwego przepływu warstwy przyściennej wokół smukłego profilu obrotowego, stosując model lepkości wirowej dla naprężenia Reynoldsa. Nieustalony charakter przepływu wprowadzono, przyjmując zmienność czasową strumienia swobodnego. Nieliniowe równanie różniczkowe o trzech zmiennych opisujące przepływ rozwiązano numerycznie za pomocą schematu różnic skończonych wprowadzonego przez Kellera. Stwierdzono, że prędkość strumienia swobodnego wpływa istotnie na charakter przepływu w warstwie przyściennej. Kąt fazowy między ścinaniem na ścianie a prędkością strumienia swobodnego jest o wiele mniejszy od kąta między grubością odpowiadającą stracie wydatku a prędkością strugi swobodnej. Współczynnik tarcia powierzchniowego maleje ze wzrostem odległości mierzonej wzdłuż prądu i z parametrem krzywizny poprzecznej przy wzroście liczby Reynoldsa. Krzywizna poprzeczna wpływa w dużym stopniu na kąt między ścinaniem na ścianie a fluktuacjami prędkości strumienia swobodnego, natomiast jej wpływ na drugi kąt fazowy jest niewielki.

Обсуждена проблема турбулентного несжимаемого течения пограничного слоя вокруг тонкого вращательного профиля, применяя модель вихревой вязкости для напряжения Рейнольдса. Неустойчивый характер течения введен, принимая временную переменность свободного потока. Нелинейное дифференциальное уравнение с тремя переменными, описывающее течение, решено численно при помощи схемы конечных разностей введенной Келлером. Констатировано, что скорость свободного потока влияет существенным образом на характер течения в пограничном слое. Фазовый угол между сдвигом на стенке и скоростью свободного потока на много меньше чем угол между толщиной, отвечающей потере потока массы, и скоростью свободной струи. Коэффициент поверхностного трения убывает с ростом расстояния измеряемого вдоль тока и с параметром поперечной кривизны при росте числа Рейнольдса. Поперечная кривизна влияет в большой степени на фазовый угол между сдвигом на стенке и флуктуациями скорости свободного потока, ее же влияние на второй фазовый угол небольшое.

### Notations

- $A$  Van Driest damping parameter,
- $A_1, B, c, c_1$  constants,
- $b$  dimensionless eddy-viscosity parameter,

$C_f$	surface skin-friction coefficient,
$f, \bar{f}$	dimensionless stream functions,
$f'$	dimensionless velocity in the $x$ -direction,
$f_w''$	skin-friction parameter,
$H$	shape factor,
$L, L_1$	reference length and mixing length, respectively,
$p_1^+$	dimensionless pressure gradient parameter,
$P$	time period,
$P_1$	function of $x$ and $t$ ,
$r$	radial distance from the axis of revolution,
$r_0$	radius of body of revolution,
$R$	transverse curvature parameter defined in Eqs. (12) <sub>3,4</sub>
$Re_x, Re_\theta$	Reynolds numbers defined with respect to $x$ and $\theta$ , respectively,
$t, t^*$	time and transformed time, respectively,
$\bar{t}$	transverse curvature function defined in Eqs. (12) <sub>3,4</sub> ,
$u, v$	velocity components in the $x$ and $y$ directions, respectively,
$u_0$	value of $u_e$ at $t = 0$ ,
$u_\tau$	friction velocity,
$x, y$	distances along and perpendicular to the surface,
$\alpha$	parameter in the outer eddy-viscosity formula,
$\gamma$	intermittency factor,
$\delta^*, \theta$	displacement and momentum thicknesses, respectively, angle (see Fig. 1),
$\bar{\theta}$	angle (see Fig. 1),
$\varepsilon_m, \varepsilon_m^+$	dimensional and dimensionless eddy-viscosities, respectively,
$\eta, \bar{\eta}, \xi$	transformed coordinates,
$\mu, \nu$	viscosity and kinematic viscosity, respectively,
$\rho$	density,
$\tau_w$	total shear stress at the wall,
$\tau_1, \tau_2$	shear stresses due to laminar and turbulent boundary layers, respectively,
$\varphi$	phase angle between $u_e$ and $f_w''$ ,
$\varphi_1$	phase angle between $\sigma^*$ and $u_e$ ,
$\psi$	dimensional stream function,
$\omega$	frequency parameter,

### Subscripts

$e, w$	conditions at the edge of the boundary layer and at the wall, respectively,
$i, 0$	inner and outer regions, respectively,
$t, x, y$	derivatives with respect to $t, x, y$ , respectively,
$\infty$	conditions in the free stream,

### Superscript

' prime denotes derivatives with respect to  $\eta$ .

## 1. Introduction

THE STUDY of unsteady turbulent boundary layers is of great interest from both theoretical and practical points of view. The effect of time dependence on the turbulent boundary layers is found to be crucial in flows over blades in compressors and turbines, on the aerodynamic surfaces of vehicles in maneuvering flight, in the flow over helicopter rotor in

translating motion etc. In recent years, there have been published several studies dealing with unsteady turbulent boundary layers. In these studies either the eddy-viscosity mixing-length concepts to model the Reynolds stresses [1—6] or the approach advocated by BRADSHAW [7] have been used. As far as the authors are aware, the unsteady incompressible turbulent boundary layer flow over a slender body of revolution has been studied so far, although the analogous steady case has been considered by several authors [8—11].

In the present paper, the unsteady incompressible turbulent boundary-layer flow over (a slender body of revolution has been studied using eddy-viscosity model valid for thick axisymmetric turbulent boundary layers. The governing partial differential equations with three independent variables have been solved numerically using an implicit finite-difference scheme developed by KELLER [12]. The results have been compared with both the theoretical and experimental results.

**2. Governing equations and eddy-viscosity model**

Let us consider an unsteady incompressible turbulent flow past an axisymmetric slender body with transverse curvature effects (see Fig. 1). We assume that there is a time-depen-

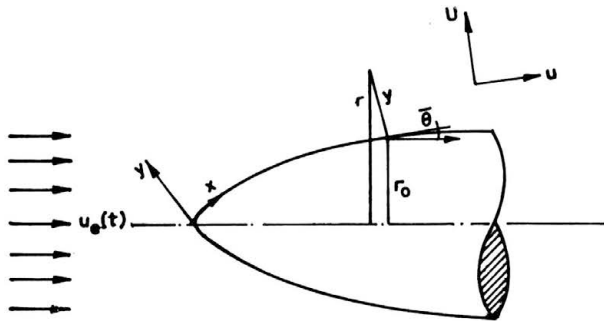


FIG. 1. Schematic diagram of a body and coordinate system.

dent axial flow in the free stream  $u_e(t)$ . The governing boundary layer equations for the velocity field are [5, 10, 11]

$$(1) \quad (ru)_x + (rv)_y = 0,$$

$$(2) \quad u_t + uu_x + vv_y = (\rho r)^{-1}(r\tau)_y + (u_e)_t,$$

where

$$(3) \quad \tau = \tau_1 + \tau_2 = \mu u_y - \rho \overline{u'v'}, \quad r = r_0 + y \cos \bar{\theta}, \quad \bar{\theta} \ll 1.$$

The initial and boundary conditions are given by

$$(4) \quad u(x, y, 0) = u_i(x, y), \quad v(x, y, 0) = v_i(x, y),$$

$$u(x, 0, t) = v(x, 0, t) = 0, \quad u(x, \infty, t) = u_e(t).$$

Here, we have used the eddy-viscosity concept which relates Reynolds shear stress  $-\rho \overline{u'v'}$  to mean velocity gradient  $u_y$  by [5, 11, 13]

$$(5) \quad -\rho \overline{u'v'} = \rho \epsilon_m u_y.$$

It may be remarked that the eddy-viscosity  $\varepsilon$  has the same units as the kinematic viscosity  $\nu$  for laminar flows. But  $\varepsilon_m$  is a function of the velocity field unlike  $\nu$  which is a property of the fluid. Hence its variation with velocity field can be obtained empirically from experimental data. In the above formulation, the turbulent boundary layer is treated as a composite layer consisting of inner and outer regions with a separate eddy-viscosity formula for each region. The expression for  $\varepsilon_m$  in the inner region is given by [11]

$$(6) \quad (\varepsilon_m)_i = L_1^2 (r/r_0) u_y,$$

where

$$(7) \quad \begin{aligned} L_1 &= 0.4r_0 \ln(r/r_0) \{1 - \exp[-(r_0/A) \ln(r/r_0)]\}, \\ A &= 26\nu u_\tau^{-1} (1 - 11.8p_i^+)^{-1/2}, \quad u_\tau = (\tau_w/\rho)^{1/2}, \\ \tau_w &= \mu(u_y)_w, \quad p_i^+ = (\nu/u_\tau^2)(u_e)_i. \end{aligned}$$

In the outer region the expression for  $\varepsilon_m$  is written in the form

$$(8) \quad (\varepsilon_m)_o = 0.0168u_e \delta^* \gamma,$$

where

$$(9) \quad \begin{aligned} \gamma &= 1.55/(1 + \alpha), \quad \alpha = 0.55[1 - \exp(-0.243z_1^{1/2} - 0.298z_1)], \\ z_1 &= (\text{Re}_\theta/425) - 1, \quad \text{Re}_\theta = u_0 \theta/\nu, \\ \delta^* &= \int_0^\infty (r/r_0)(1 - u/u_e) dy, \quad \theta = \int_0^\infty (r/r_0)(u/u_e)(1 - u/u_e) dy. \end{aligned}$$

Here  $x$  and  $y$  are the distances along and perpendicular to the surface;  $u$  and  $v$  are the velocity components in the  $x$  and  $y$  directions, respectively;  $t$  is the time;  $r$  is the radial distance from the axis of revolution;  $r_0$  is the radius of body of revolution;  $\theta$  is the angle which the tangent to the meridian profile makes with the body axis;  $\rho$  is the density;  $\mu$  is the coefficient of viscosity;  $\tau$  is the shear stress and  $\tau_1$  and  $\tau_2$  are its contribution due to laminar and turbulent boundary layers, respectively;  $u_0$  is the free stream velocity  $u_e$  at  $t = 0$ ;  $\varepsilon_m$  is the eddy-viscosity and  $(\varepsilon_m)_i$  and  $(\varepsilon_m)_o$  are its values in the inner and outer regions of turbulent boundary layers.  $\gamma$  is the intermittency factor;  $L_1$  is the mixing length;  $A$  is the Van Driest damping parameter;  $u_\tau$  is the frictional velocity;  $\nu$  is the kinematic viscosity;  $p_i^+$  is the dimensionless pressure gradient parameter;  $\delta^*$  and  $\theta$  are the displacement and momentum thicknesses, respectively;  $\text{Re}_\theta$  is the Reynolds number defined with respect to  $\theta$ ; the subscripts  $t$ ,  $x$  and  $y$  denote partial derivatives with respect to  $t$ ,  $x$  and  $y$ , respectively; the subscript  $i$  denotes the initial conditions and the subscripts  $e$  and  $w$  denote conditions at the edge of the boundary layer and on the surface, respectively.

It may be remarked that here we have considered the unsteady incompressible turbulent boundary layer flow over a slender body of revolution without mass transfer ( $v_w = 0$ ) when the velocity at the edge of the boundary layer  $u_e$  depends on time  $t$  only (i.e.  $u_e = u_e(t)$ ). This problem is different from those studied by CEBECI in Refs. [5, 11]. The Van Driest damping parameter  $A$  in our equation (7) is identical to that of Ref. [5] if we put  $p_x^+ = 0(p_x^+ = \nu u_\tau^{-3} \times u_e(u_e)_x)$  in Eq. (6) of Ref. [5], because  $(u_e)_x = 0$  since  $u_e$  is a function of  $t$  only. It also reduces to that of Ref. [11] if we put  $p_i^+ = 0$  in our equation (7) and also put  $v_w^+ = 0(v_w^+ = v_w/u_\tau)$ ,  $p^+ = 0(p^+ = -(\nu/\rho u_\tau) p_x)$  in Eq. (4) of Ref. [11]. This

implies that  $N = 1$  in Eq. (4) of Ref. [11]. It may be noted that CEBECI has given the Van Driest damping parameter  $A$  in Eq. (4) of Ref. [11] for steady compressible turbulent boundary layer flow with mass transfer which is different from the problem considered here.

Applying the following transformations

$$(10) \quad \begin{aligned} \xi &= \rho\mu u_0(r_0/L)^2 x, & \eta &= \rho u_0(2\xi)^{-1/2}(r/L)y, \\ t^* &= \rho\mu u_0(r_0/L)^2 t, & (r/L)u &= \psi_y, & -(r/L)v &= \psi_x, \\ \psi &= (2\xi)^{1/2}f(\xi, \eta, t^*), & u &= u_0 f', \\ -v &= (2\xi)^{-1/2}(L/r)\rho\mu u_0(r_0/L)^2 [f + 2\xi f_\xi - \eta f'], \end{aligned}$$

to Eq. (1), we find that it is identically satisfied and (2) reduces to

$$(11) \quad [b(1+\bar{t})^2 f'']' + f f'' + P_1 = 2x(f' f'_x - f'' f_x + u_0^{-1} f'_t),$$

where

$$(12) \quad \begin{aligned} b &= 1 + \varepsilon_m^+, & \varepsilon_m^+ &= \varepsilon_m/\nu & (\varepsilon_m = (\varepsilon_m)_i \text{ or } (\varepsilon_m)_o), \\ P_1 &= (2x/u_0^2)(u_e)_t, & (r/r_0) &= 1 + \bar{t}, \\ \bar{t} &= (y/r_0) = [1 + (2/R)^{1/2}\eta]^{1/2} - 1, & \xi(\partial/\partial\xi) &= x(\partial/\partial x), \\ R &= (\text{Re}_x/4)(r_0/x)^2, & \text{Re}_x &= u_0 x/\nu, & \xi(\partial/\partial t^*) &= x(\partial/\partial t). \end{aligned}$$

The boundary conditions are given by

$$(13) \quad \begin{aligned} f &= f' = 0 & \text{at} & \eta = 0, \\ f' &= u_e/u_0 & \text{as} & \eta \rightarrow \infty, & t \geq 0, & x \geq 0. \end{aligned}$$

The initial conditions at  $t = 0$  can be obtained from Eq. (11) by putting  $t = f'_t = p_t^+ = P_1 = 0$  in it. Similarly, the initial conditions at  $x = 0$  can be obtained from Eq. (11) by putting  $x = 0$  in it and they are given by

$$(14) \quad \begin{aligned} [b(1+\bar{t})^2 f'']' + f f'' &= 2x(f' f'_x - f'' f_x), \\ [b(1+\bar{t})^2 f'']' + f f'' &= 0. \end{aligned}$$

It may be noted that at  $t = 0$ , the flow can be either laminar or turbulent. In the latter case the surface distance  $x$  must be greater than zero [5]. The governing Eq. (11) also reduces to that of the flat plate case which was studied by CEBECI [5] if we put  $\eta = 2^{1/2} \bar{\eta}$  and  $f = 2^{-1/2} \bar{f}$  in it.

Using Eq. (6) to (9), the dimensionless eddy-viscosity  $\varepsilon_m$  both in the inner and outer regions can be expressed in the form

$$(15) \quad \varepsilon_m^+ = \begin{cases} (\varepsilon_m)_i^+ = 0.16(2)^{3/2}(r/r_0)^2 R \text{Re}_x^{1/2} f'' [\ln(r/r_0)]^2 (1 - \exp\{- (r_0/A) \ln(r/r_0)\})^2, \\ (\varepsilon_m)_o^+ = 0.0168(2 \text{Re}_x)^{1/2} \gamma(\eta_\infty - f_\infty), \end{cases}$$

where

$$(15') \quad r_0/A = (1/26)(f'_w)^{1/2}(8R^2 \text{Re}_x)^{1/4}(r/r_0)^2(1 - 11.8p_t^+).$$

The skin friction coefficient can be written as

$$(16) \quad C_f = 2\tau_w/\rho u_0^2 = (2/\text{Re}_x)^{1/2} f'_w.$$

From Eq. (9)<sub>2</sub>, the displacement and momentum thicknesses and shape factor are given by

$$(17) \quad \delta^* = (2/\text{Re}_x)^{1/2} x [\eta_\infty^- - (f_\infty/f'_\infty)], \quad H = \delta^*/\theta,$$

$$\theta = (2/\text{Re}_x)^{1/2} x \int_0^\infty (f'/f'_\infty) [1 - (f'/f'_\infty)] d\eta.$$

Here  $\xi$  and  $\eta$  are transformed coordinates;  $L$  is the reference length,  $t^*$  is the transformed time;  $\psi$  and  $f$  are the dimensional and dimensionless stream functions, respectively;  $f'$  is the dimensionless velocity in the boundary layer;  $\varepsilon_w^+$  is the dimensionless eddy-viscosity;  $b$  is the dimensionless eddy-viscosity parameter;  $P_1$  is a function of  $x$  and  $t$ ;  $\bar{t}$  is transverse curvature function;  $R$  is the transverse curvature parameter;  $\text{Re}_x$  is the Reynolds number with respect to  $x$ ;  $f_w''$  and  $C_f$  are the skin friction parameter and coefficient, respectively; and  $H$  is the shape factor; and the subscript  $\infty$  denotes the conditions at the edge of the boundary layer. The prime denotes derivatives with respect to  $\eta$ .

For fluctuating free stream velocity distribution  $u_e(t) = u_0(1 + B\cos\omega t)/(1 + B)$ , the phase angle between the free stream velocity  $u_e$  and the surface skin friction parameter  $f_w''$  for a fixed value of  $x = x_0$  can be obtained by following the analysis of CEBECI [5, 13]. The phase angle  $\varphi$  is given by

$$(18) \quad \cos\varphi(x_0) = (Ac\pi/\omega)^{-1} \int_{t_0}^{t_0+P} [u_e(t) - (1+B)^{-1}u_0] [f_w''(x_0, t) - \overline{f_w''(x_0)}] dt,$$

where

$$(19) \quad u_0 = (1+B)P^{-1} \int_{t_0}^{t_0+P} u_e(t) dt, \quad P = 2\pi/\omega,$$

$$\overline{f_w''(x_0)} = P^{-1} \int_{t_0}^{t_0+P} f_w''(x_0, t) dt, \quad t_0 = P,$$

$$u_e(t) - (1+B)^{-1}u_0 = A\cos\omega t, \quad A = u_0B/(1+B),$$

$$f_w''(x_0, t) - \overline{f_w''(x_0)} = c\cos[\omega t + \varphi(x_0)],$$

$$A^2 = (\omega/\pi) \int_{t_0}^{t_0+P} [u_e(t) - u_0(1+B)^{-1}]^2 dt,$$

$$c^2 = (\omega/\pi) \int_{t_0}^{t_0+P} [f_w''(x_0, t) - \overline{f_w''(x_0)}]^2 dt.$$

Here  $\omega$  is the frequency parameter and  $B$  is a constant. Similarly, the phase angle  $\varphi_1$  between displacement thickness  $\delta^*$  and external velocity (i.e. between  $\delta^*$  and  $u_e$ ) is given by

$$(20) \quad \cos\varphi_1(x_0) = (Ac_1\pi/\omega)^{-1} \int_{t_0}^{t_0+P} [u_e(t) - (1+B)^{-1}u_0] [\delta^*(x, t) - \overline{\delta^*(x_0)}] dt,$$

where

$$\begin{aligned} \overline{\delta^*(x_0)} &= P^{-1} \int_{t_0}^{t_0+P} \delta^*(x_0, t) dt, \\ c_1^2 &= (\omega/\pi) \int_{t_0}^{t_0+P} [\delta^*(x_0, t) - \overline{\delta^*(x)}]^2 dt. \end{aligned} \tag{21}$$

Following the procedure of CEBECI [5, 13], the in-phase and out-of-phase velocity components denoted by  $\overline{A}$  and  $\overline{B}$ , respectively, can be written in the form

$$\begin{aligned} \overline{A}(\eta) &= \frac{u^{(1)} \cos \varphi}{u_\infty^{(1)}} = \frac{\omega}{2\pi} \frac{(1+B)}{B} \int_0^{2\pi/\omega} f'(\eta, t) \cos \omega t dt, \\ \overline{B}(\eta) &= \frac{u^{(1)} \sin \varphi}{u_\infty^{(1)}} = -\frac{\omega}{2\pi} \frac{(1+B)}{B} \int_0^{2\pi/\omega} f'(\eta, t) \sin \omega t dt, \end{aligned} \tag{22}$$

where

$$\begin{aligned} u_0 f' &= \bar{u}(x, y) + u^{(1)} \cos \varphi \cos \omega t - u^{(1)} \sin \varphi \sin \omega t, \\ u_e &= u_0(1 + B \cos \omega t)/(1 + B), \quad u_\infty^{(1)} = u_0 B/(1 + B). \end{aligned} \tag{23}$$

### 3. Results and discussion

The governing equation (11) has been solved numerically under the boundary conditions (13) and initial conditions (14) with relations given in (15), using an implicit finite-difference scheme developed by KELLER [12]. Since the detailed description of the method for three independent variables is given in [5, 13, 14], for the sake of brevity, its description is omitted here. Here, we have studied the effect of step sizes  $\Delta\eta$ ,  $\Delta x$  and  $\Delta t$  and  $\eta_\infty$  (edge of the boundary layer) on the solution with a view to optimize them. Subsequently, we have carried out the computation with  $\Delta t = 0.2$  and  $\Delta x = 0.1$  and  $0.15$  as the first and second step size. For  $x > 0.25$ ,  $\Delta x = 0.25$  has been used. We have used the non-uniform step in the  $\eta$  direction because the boundary layer thickness is large for turbulent flows and the gradient of velocity at/or near the wall is quite high as compared to laminar flows. Hence, to get a better accuracy, small step size is required while large step size can be used away from the wall. Initially, the edge of the boundary layer  $\eta_\infty$  was taken as 6 with  $\Delta\eta = 0.1$ . During the calculation  $\eta_\infty$  was allowed to grow. The detailed description of the variable step size is given by CEBECI and SMITH [15]. The results presented here are found to be independent of the step size and  $\eta_\infty$  at least up to the 4th decimal place. For computation, two types of free stream velocity distributions have been used: (I) a fluctuating flow given by  $u_e = u_0(1 + B \cos \omega t)/(1 + B)$  and (II) an accelerating flow represented by  $u_e = u_0[1 + (t/\varepsilon)^2]$ , where  $\varepsilon$  has a dimension  $t$  ( $t$  is measured in sec). The present method of solution is valid for both the laminar and turbulent flows; here it is assumed to be laminar and turbulent flows; here it is assumed to be laminar at  $x = 0$  and considered to be turbulent at  $x > 0$  (say  $x = 0.1$ ). We also find that the method is extremely efficient and a typical data takes about 20.75 sec CPU time on DEC-1090 computer.

**Table 1.** Comparison of skin-friction for steady laminar flow.

$R$	$C_f(\text{Re}_x)^{1/2}$	
	Present calculation	CEBECI [9]
1000	0.6868	0.6867
100	0.7292	0.7305
10	0.8597	0.8600
1	1.1913	1.1910
0.1	2.0048	2.0086
0.01	3.9657	3.9699
0.001	9.1199	9.1293

In order to assess the accuracy of our method, we have compared our skin friction results ( $C_f(\text{Re}_x)^{1/2}$ ) for steady laminar flow with those of CEBECI [9]. The comparison is given in Table 1. We have also compared our skin friction results ( $C_f$ ) for steady turbulent flow with the experimental results of RICHMOND [8], the theoretical results of WHITE [10]

**Table 2.** Comparison of skin friction coefficient for steady turbulent flow for  $u_e = u_0$ ,  $u_0 = 5.33$  m/s,  $\nu = 2.09 \times 10^{-5}$  m<sup>2</sup>/s.

$d(= 2r_0)$ cm	$\text{Re}_0$	$C_f \times 10^3$			
		Present calculation	CEBECI [11]	RICHMOND [8]	WHITE [10]
0.06096	2100	8.215	8.21	4.95	7.71
0.0254	8750	3.016	3.02	2.90	3.18

**Table 3.** Phase angle between wall shear and oscillating external velocity for  $u_0 = 5.33$  m/s,  $B = 0.147$ ,  $\omega = 1.57$  rad/s,  $\nu = 2.09 \times 10^{-5}$  m<sup>2</sup>/s.

$\frac{\omega_x}{u_0}$	$\varphi$					
	$R = 0.001$		$R = 1$		$R = 1000$	
	One cycle	Two cycles	One cycle	Two cycles	One cycle	Two cycles
0.147	1.16	1.12	1.88	1.86	3.69	3.66
0.295	1.22	1.21	2.49	2.53	4.99	5.00
0.589	1.45	1.42	2.52	2.56	6.45	6.56
1.178	1.76	1.70	2.68	2.67	8.51	8.52
1.767	1.77	1.74	2.61	2.72	9.50	9.51
2.356	1.79	1.80	2.89	2.64	10.30	10.25
2.946	1.79	1.76	3.16	3.15	10.91	10.62
3.240	1.75	1.79	3.10	3.15	11.04	10.72
3.535	1.77	1.74	3.19	3.16	11.12	10.76
3.829	1.71	1.75	3.19	3.25	11.20	10.74
4.124	1.74	1.72	3.25	3.29	11.25	10.73
4.418	1.73	1.74	3.65	3.64	11.29	10.68



**Table 4. Phase angle between displacement thickness and oscillating external velocity for  $u_0 = 5.35$  m/s,  $B = 0.147$ ,  $\omega = 1.57$  rad/s,  $\nu = 2.09 \times 10^{-5}$  m<sup>2</sup>/s.**

$\frac{\omega x}{u_0}$	$\varphi_1$					
	$R = 0.001$		$R = 1$		$R = 1000$	
	One cycle	Two cycles	One cycle	Two cycles	One cycle	Two cycles
0.147	169.24	169.42	170.56	169.47	133.69	133.67
0.295	169.90	169.99	169.94	169.80	143.27	142.24
0.589	169.03	168.92	160.10	160.71	141.64	141.74
1.178	166.95	168.43	167.82	168.38	140.28	140.63
1.767	167.91	169.29	165.45	165.90	140.68	141.53
2.356	169.10	169.90	163.33	163.55	141.59	142.97
2.946	169.65	170.03	162.25	162.45	141.78	144.02
3.240	170.57	170.35	161.57	161.78	142.33	144.55
3.535	169.73	170.23	160.97	161.08	142.81	145.15
3.829	170.35	170.22	160.41	160.52	143.36	146.24
4.124	170.33	170.26	160.03	160.14	143.83	147.10
4.418	170.36	170.42	160.34	160.09	144.32	147.89

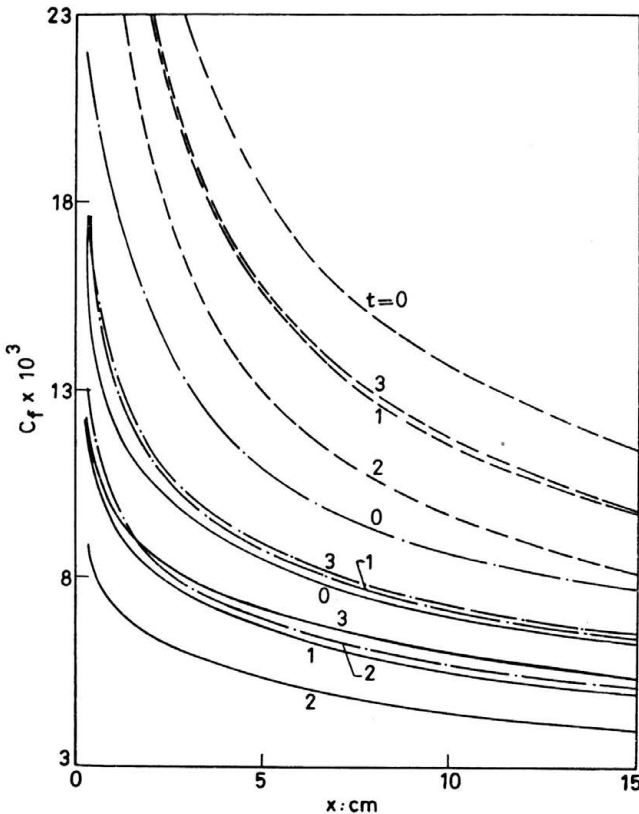


**FIG. 2. Skin-friction coefficient  $C_f \times 10^3$  for  $u_e = u_0(1 + B \cos \omega t)/(1 + B)$ ,  $u_0 = 5.35$  m/s,  $B = 0.147$ ,  $\omega = 1.57$  rad/s,  $\nu = 2.09 \times 10^{-5}$  m<sup>2</sup>/s ———,  $R = 1000$ ; — · — · —,  $R = 1$ ; — — —,  $R = 0.001$ .**

and CEBECI [11]. The comparison is presented in Table 2. In both cases, the results are found to be in excellent agreement.

For turbulent flow, the variation of the phase angle  $\varphi$  between wall shear  $f''_w$  and the external velocity  $u_e = u_0(1+B\cos\omega t)/(1+B)$  with reduced frequency  $(\omega x/u_0)$  for two cycles and for three values of transverse curvature parameter ( $R$ ) is given in Table 3. Similarly, Table 4 gives the variation of the phase angle  $\varphi_1$  between displacement thickness and the external velocity  $u_e = u_0(1+B\cos\omega t)/(1+B)$  with reduced frequency  $(\omega x/u_0)$ . It is observed that in both cases the results differ very little from one cycle to another. Similar trend has been observed by CEBECI [8, 13] for unsteady flat plate case. We also observe that the phase angle  $\varphi$  between  $f''_w$  and  $u_e$  is much smaller than the phase angle  $\varphi_1$  between  $\delta^*$  and  $u_e$ . The effect of transverse curvature  $R$  is found to be more pronounced on  $\varphi$  than on  $\varphi_1$ .

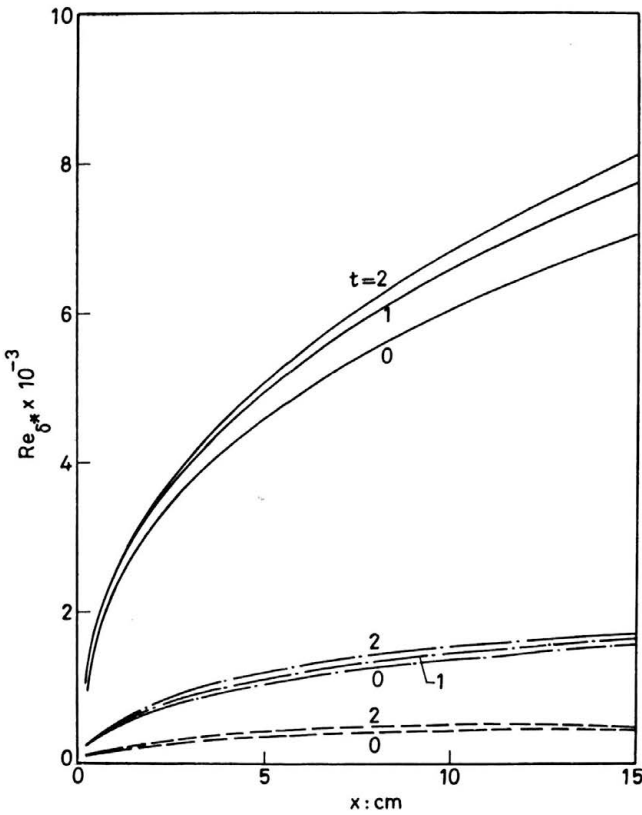


FIG. 3. Reynolds number with respect to  $\delta^*$ ,  $Re_{\delta^*} \times 10^{-3}$ , for  $u_e = u_0 (1+B\cos\omega t)/(1+B)$ ,  $u_0 = 5.33$  m/s,  $B = 0.147$ ,  $\omega = 1.57$  rad/s,  $\nu = 2.09 \times 10^{-5}$  m<sup>2</sup>/s. ———,  $R = 1000$ ; — · — · —,  $R = 1$ ; - - - - -,  $R = 0.001$ .

The turbulent flow results for oscillatory free stream velocity  $u_e = u_0(1+B\cos\omega t)/(1+B)$  are given in Figs. 2—7 and for constantly accelerating free stream velocity  $u_e = u_0[1+(t/\epsilon)^2]$  in Fig. 8.

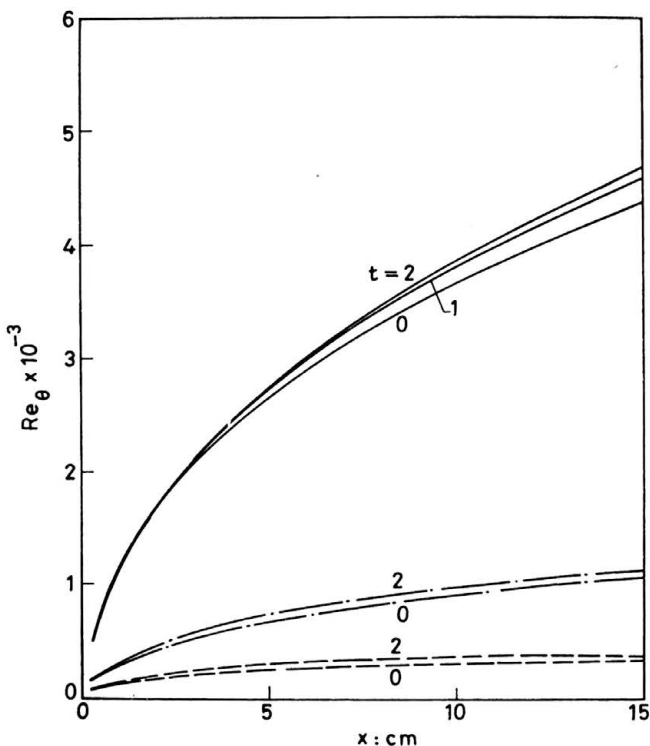


FIG. 4. Reynolds number with respect to  $\theta$ ,  $Re_\theta \times 10^{-3}$ , for  $u_e = u_0(1 + B \cos \omega t)/(1 + B)$ ,  $u_0 = 5.33$  m/s,  $B = 0.147$ ,  $\omega = 1.57$  rad/s,  $\nu = 2.09 \times 10^{-5}$  m<sup>2</sup>/s ———,  $R = 1000$ ; — · — · —,  $R = 1$ ; — — — —,  $R = 0.001$ .

Figures 2 to 5, respectively, give the variation of skin-friction coefficient ( $C_f$ ),  $Re_{\delta^*}$ ,  $Re_\theta$  and  $H$  (where  $Re_{\delta^*}$  and  $Re_\theta$  are the Reynolds numbers defined, respectively, with respect to  $\delta^*$  and  $\theta$ , and  $H = \delta^*/\theta$  is the shape factor) with the streamwise distance  $x$  for several values of  $t$  and  $R$ . It is observed that the skin-friction coefficient ( $C_f$ ) decreases rapidly with  $x$  in the range  $0 < p < 10$  (Fig. 2). However, the change is small when  $x \geq 10$ . For given  $x$  and  $t$ ,  $C_f$  also decreases as the transverse curvature parameter  $R$  increases, but for a prescribed  $x$  and  $R$ ,  $C_f$  oscillates with time  $t$ . The Reynolds numbers  $Re_{\delta^*}$  and  $Re_\theta$  increase with  $p$  and  $R$ , whereas  $H$  decreases with  $x$ , but increases with  $R$  except when  $R = 0.10^{-3}$ . However, they all oscillate with  $t$ . It may be remarked that the reduction in the skin friction coefficient  $C_f$  as  $x$  and (or)  $R$  increase is due to the increase in the boundary layer thickness. Similarly, the oscillatory behaviour of  $C_f$  with time  $t$  is due to its response to the free stream velocity which also oscillates with  $t$ .

Figure 6 shows the in-phase and the out-of-phase components of velocity ( $\bar{A}(\eta)$ ,  $\bar{B}(\eta)$ ) for two values of  $x$ . It is found that the in-phase component of velocity  $\bar{A}(\eta)$  increases with  $\eta$  and tends to 1 whereas the out-of-phase component of velocity  $\bar{B}(\eta)$  first increases with  $\eta$  in the range  $(0 \leq \eta < 2.3)$  and then rapidly decreases.

The velocity profile  $f'$  for different values of transverse curvature parameter  $R$  and streamwise distance  $x$  is given in Fig. 7. The velocity profile becomes very steep as the

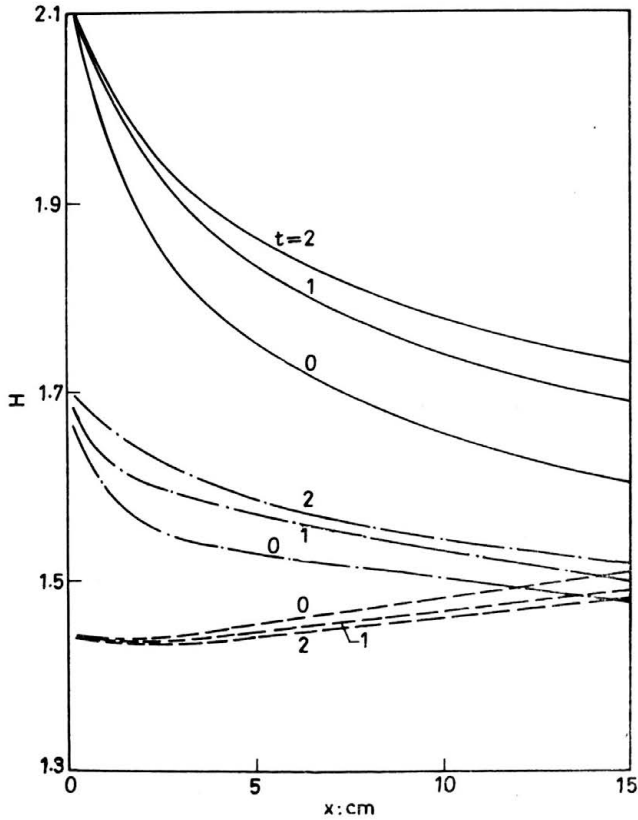


FIG. 5. Shape factor  $H$  for  $u_e = u_0(1+B\cos\omega t)/(1+B)$   $u_0 = 5.33$  m/s,  $B = 0.147$ ,  $\omega = 1.57$  rad/s,  $\nu = 2.09 \times 10^{-5}$  m<sup>2</sup>/s, ———,  $R = 1000$ ; — · — · —,  $R = 1$ ; - - - - - ,  $R = 0.001$ .

transverse curvature  $R$  decreases due to higher wall shear. However, the profile  $f'$  becomes less steep as  $x$  increases.

The results ( $C_f$ ,  $Re_{\delta^*}$ ,  $Re_\theta$ ,  $H$ ) for accelerating flow ( $u_e = u_0(1+\varepsilon^{-2}t^2)$ ) are given in Fig. 8. The skin-friction coefficient  $C_f$  is found to increase with  $t$ , whereas  $Re_{\delta^*}$ ,  $Re_\theta$  and  $H$  decrease. However, their behaviour with  $x$  is found to be qualitatively similar to those of the oscillatory case.

#### 4. Conclusions

It is observed that the boundary layer characteristics are strongly affected by the free stream velocity. The skin-friction coefficient is found to decrease as the transverse curvature parameter and streamwise distance increase. The transverse curvature strongly affects the phase angle between wall shear and fluctuating free stream velocity, but its effect on the phase angle between displacement thickness and fluctuating free stream velocity is small.

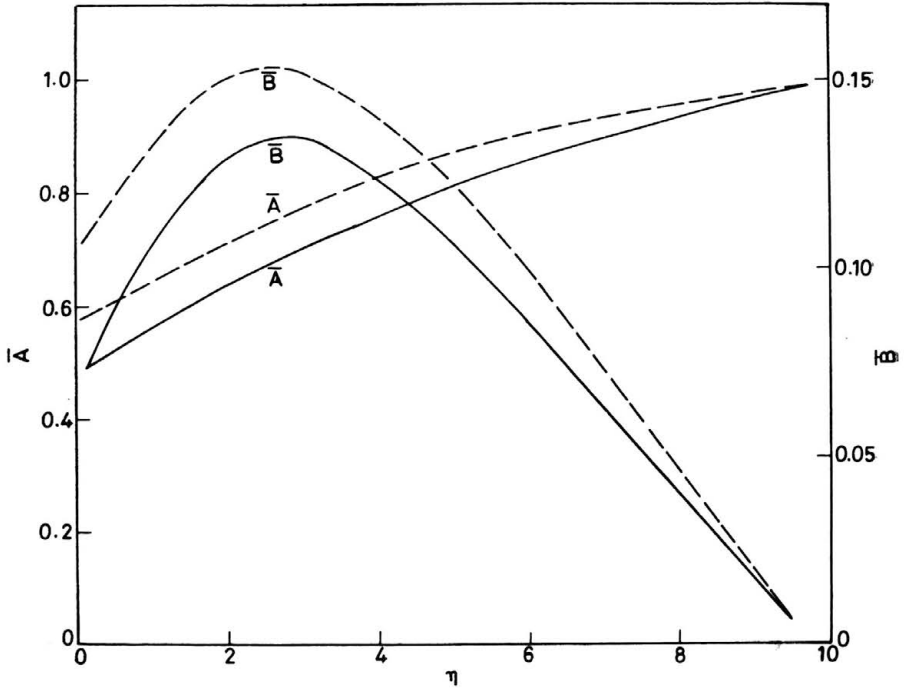


FIG. 6. In-phase component  $\bar{A}$  and out-of-phase component  $\bar{B}$  of velocity for  $u_e = u_0(1 + B\cos\omega t)/(1 + B)$ ,  $u_0 = 5.33$  m/s,  $B = 0.147$ ,  $\omega = 1.57$  rad/s,  $\nu = 2.09 \times 10^{-5}$  m<sup>2</sup>/s ———,  $x = 5$  cms; - - - - -,  $x = 10$  cms.

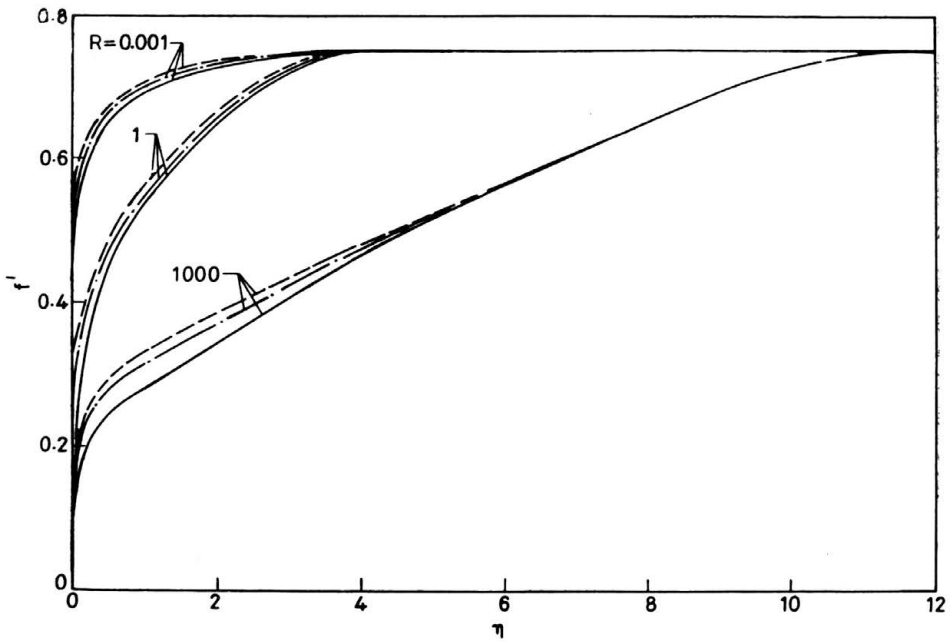


FIG. 7. Velocity profile  $f'$  for  $u_e = u_0(1 + B\cos\omega t)/(1 + B)$ ,  $u_0 = 5.33$  m/s,  $B = 0.147$ ,  $\omega = 1.57$  rad/s,  $\nu = 2.09 \times 10^{-5}$  m<sup>2</sup>/s,  $t = 2$ . ———,  $x = 5$  cms; — · — · —,  $x = 10$  cms; - - - - -,  $x = 15$  cms.

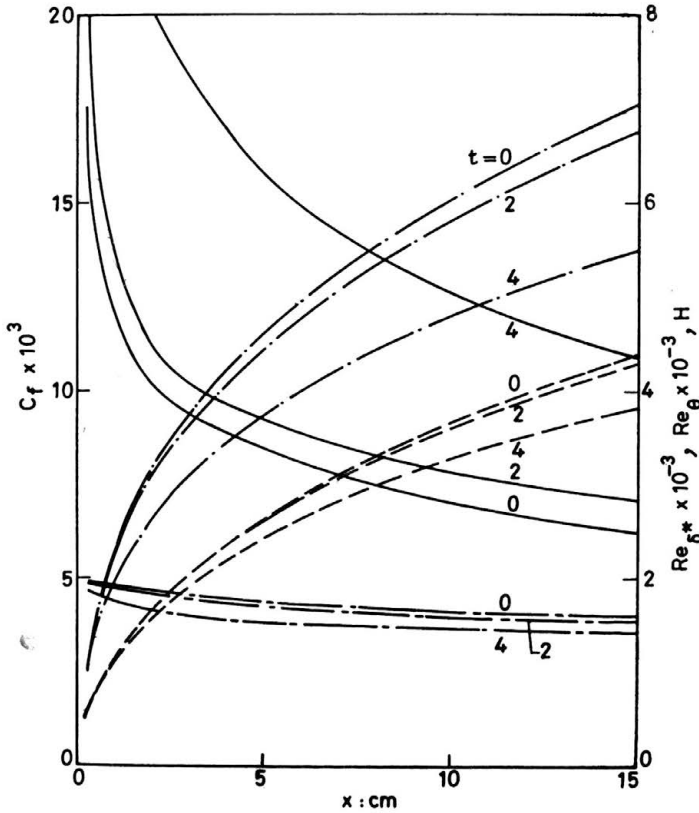


FIG. 8. Skin-friction coefficient  $C_f \times 10^3$ , Reynolds number with respect to  $\delta^*$ ,  $Re_{\delta^*} \times 10^{-3}$ , Reynolds number with respect to  $\theta$ ,  $Re_{\theta} \times 10^{-3}$ , and shape factor  $H$  for  $u_e = u_0(1 + \varepsilon^{-2}t^2)$ ,  $u_0 = 5.33$  m/s,  $\varepsilon = 6.8$  s,  $\nu = 2.09 \times 10^{-5}$  m<sup>2</sup>/s,  $R = 1000$ . ———,  $C_f \times 10^{-3}$ ; - - - - - ,  $Re_{\delta^*} \times 10^{-3}$ ; - · - · - ,  $Re_{\theta} \times 10^{-3}$ ; ·····,  $H$ .

## References

1. W. J. MCCROSKEY and J. J. PHILIPPE, *Unsteady viscous flow on oscillating airfoils*, AIAA J., **13**, 71—79, 1975.
2. D. P. TELIONIS, *Calculation of time-dependent boundary layer*, In: *Unsteady Aerodynamics*, Vol. 1 (Ed. R. B. KINNEY), The University of Arizona, 155—190, 1975.
3. J. F. NASH, L. W. CARR, and R. SINGLETON, *Unsteady turbulent boundary layers in two-dimensional incompressible flow*, AIAA J., **13**, 167—172, 1975.
4. V. C. PATEL and J. F. NASH, *Unsteady turbulent boundary layers with flow reversal*, In: *Unsteady Aerodynamics*, Vol. 1 (Ed. R. B. KINNEY), The University of Arizona, 191—220, 1975.
5. T. CEBECI, *Calculation of unsteady two-dimensional laminar and turbulent boundary layers with fluctuations in external velocity*, Proc. Roy. Soc. London, **355A**, 225—238, 1977.
6. W. L. HANKEY and W. CALERESE, *Reynolds stresses for unsteady turbulent flows*, AIAA J., **21**, 1210—1211, 1983.
7. P. BRADSHAW, *Calculation of boundary layer development using the turbulent energy equation, VI. Unsteady flow*, AERO Rept. 1288, National Physical Lab., England, Feb. 1969.

8. R. RICHMOND, *Experimental investigation of thick axially symmetric boundary layers on cylinders at subsonic and hypersonic speeds*, Ph. D. Thesis, California Institute of Technology, Pasadena 1957.
9. T. CEBECI, *Laminar and turbulent incompressible boundary layers on slender bodies of revolution in axial flow*, Trans. ASME J. Basic Engng., **92**, 545—554, 1970.
10. F. M. WHITE, *An analysis of axisymmetric turbulent flow past a long cylinder*, Trans. ASME J. Basic Engng., **94**, 200—206, 1972.
11. T. CEBECI, *Eddy-viscosity distribution in thick axisymmetric turbulent boundary layers*, Trans. ASME J. Fluids Engng., **95**, 319—326, 1973.
12. H. B. KELLER, *A new difference scheme for parabolic problems*, In: Numerical Solution of Partial Differential Equations, Vol. 2 (Ed. J. BRAMBLE), Academic Press, New York, 327—350, 1971.
13. T. CEBECI, *Calculation of laminar and turbulent boundary layers for two-dimensional time-dependent flows*, NASA CR-2820, 1977.
14. R. CEBECI and P. BRADSHAW, *Momentum transfer in boundary layers*, McGraw-Hill-Hemisphere, Washington 1977.
15. T. CEBECI and A. M. O. SMITH, *Analysis of turbulent boundary layers*, Academic Press, New York 1974.

DEPARTMENT OF APPLIED MATHEMATICS  
INDIAN INSTITUTE OF SCIENCES, BANGALORE, INDIA.

*Received February 8, 1985.*